Three-Dimensional Solution Structure of *Saccharomyces cerevisiae* Reduced Iso-1-cytochrome *c*[†]

Paolo Baistrocchi, Lucia Banci, Ivano Bertini,* and Paola Turano

Department of Chemistry, University of Florence, Via Gino Capponi 7, 50121 Florence, Italy

Kara L. Bren and Harry B. Gray*

Arthur Amos Noyes Laboratory, California Institute of Technology, Pasadena, California 91125

Received May 8, 1996[⊗]

ABSTRACT: Two-dimensional ^{1}H NMR spectra of *Saccharomyces cerevisiae* reduced iso-1-cytochrome *c* have been used to confirm and slightly extend the assignment available in the literature. 1702 NOESY cross-peaks have been assigned, and their intensities have been measured. Through the program DIANA and related protocols (Güntert, 1992), a solution structure has been obtained by using 1442 meaningful NOEs and 13 hydrogen-bond constraints. The RMSD values with respect to the mean structure for the backbone and all heavy atoms for a family of 20 structures are 0.61 ± 0.09 and 0.98 ± 0.09 Å, the average target function value being as small as 0.57 Å^2. The larger number of slowly exchanging amide NHs observed in this system compared to that observed in the cyanide derivative of oxidized Ala 80 cytochrome *c* suggests that the oxidized form is much more flexible and that the backbone protons are more solvent accessible. Comparison of the present structure with the crystal structures of reduced yeast cytochrome *c* and of the complex between cytochrome *c* peroxidase and oxidized yeast cytochrome *c* reveals substantial similarity among the backbone conformations but differences in the residues located in the region of protein−protein interaction. Interestingly, in solution the peripheral residues involved in the interaction with cytochrome *c* peroxidase are on average closer to the position found in the crystal structure of the complex than to the solid state structure of the isolated reduced form.

Cytochromes are electron transfer proteins that contain heme prosthetic groups (Moore & Pettigrew, 1990; Pettigrew & Moore, 1987), and *c*-type cytochromes contain the heme covalently bound to the protein matrix through thioether linkages involving two cysteine residues (heme *c*). Class I cytochromes *c* are characterized by the presence of a single heme *c* close to the N-terminus and by His-Met axial ligation to the iron. The iron switches its oxidation state between +2 and +3 during biological function and is always in a low-spin state.

Despite the extensive characterization of cytochrome *c* with a variety of techniques, a debate is still open on the possible conformational changes occurring upon change of the iron oxidation state and their relationship to the electron transfer process. While some investigations pointed out differences between the two oxidation states (Ulmer & Kagi, 1968; Eden et al., 1982; Moore, 1983; Trehwella et al., 1988; Liu et al., 1989), later studies indicated that the variations between the oxidized and the reduced forms are localized and do not imply conformational changes (Korszun et al., 1982; Wand et al., 1986; Feng & Englander, 1990; Feng et al., 1990). Furthermore, the X-ray crystal structures of the oxidized and reduced forms of yeast cytochrome *c* are very similar (Berghuis & Brayer, 1992). It is possible, however, that the electrostatic potential differences resulting from the different charges on the heme iron in the different oxidation states lead to some changes in the internal mobility of the protein. In turn, understanding internal mobility could help in investigations of protein folding, particularly in metal-containing proteins.

Solution structures of proteins obtained through NMR represent independent information on the structure and mobility of the backbone and the side chains of protein residues (Wüthrich, 1995; Wagner, 1990). When available, the comparison with the X-ray structure is quite informative in terms of mobility of the residues and of protein function.

Employing NMR spectroscopy, we have determined the solution structure of the reduced form of *Saccharomyces cerevisiae* iso-1-cytochrome *c*. The ultimate aim of our research on yeast cyt *c* is to obtain evidence of structural and dynamical differences between oxidized and reduced forms and among mutants (Banci et al., 1995). Here, we compare the solution and X-ray structures (Louie & Brayer, 1990; Berghuis & Brayer, 1992) of the reduced protein and comment on the mobility of the peripheral residues, paying particular attention to those involved in the interaction with cytochrome *c* peroxidase (CcP), which is one of its physiological partners (Pelletier & Kraut, 1992). We also compare the mobility of this protein with that of the cyanide derivative of the oxidized form of the Ala 80 mutant (Banci et al., 1995).

EXPERIMENTAL SECTION

Sample Preparation. Yeast iso-1-cytochrome *c* with serine at position 102 (Cys102Ser) was expressed and purified as

[†] This work was supported by CNR (Italy) and NSF (U.S.A.); it was performed with the instrumentation of the Florence Laboratory of Relaxometry and Magnetic Resonance on Paramagnetic Metalloproteins, Large Scale Facility of the European Community (Contract No. ERBCHGECT940060).

* Corresponding author: Department of Chemistry, University of Florence, Via Gino Capponi 7, 50121 Florence, Italy. Tel: +39-55-275 7549. FAX: +39-55-275 7555.

[⊗] Abstract published in *Advance ACS Abstracts,* October 1, 1996.

S0006-2960(96)01110-5 CCC: $12.00

previously reported (Lu et al., 1993). The ^{1}H NMR samples (in H_2O and in D_2O) were prepared by dissolving the lyophilized protein in 50 mM phosphate buffer at pH 7.0 to give 3 mM solutions. The pH of protein samples prepared for NMR spectroscopy was adjusted by addition of small volumes of concentrated solutions of NaOH and H_3PO_4. The pH was measured (uncorrected for the isotope effect) with an Orion model 720 pH meter and a Microelectrodes, Inc. model MI-410 microcombination pH probe.

NMR Spectra. NMR spectra were acquired on a Bruker AMX 600 MHz spectrometer. TPPI NOESY (Macura et al., 1982; Marion & Wüthrich, 1983) spectra were recorded with presaturation of the solvent signal both during the relaxation delay and the mixing time to eliminate the water signal. NOESY maps at 295 and 303 K in D_2O solution (90%D_2O/10%H_2O) were recorded with recycle times of 800 ms and mixing times of 100 ms. Analogously, clean-TOCSY (Bax & Davis, 1985; Griesinger et al., 1988) experiments were recorded with recycle times of 800 ms and spin-lock times of 90 ms. A DQF COSY (Rance et al., 1983) map was recorded in H_2O solution on a 30 ppm spectral width (recycle time 800 ms). NOESY and TOCSY maps in H_2O using the WATERGATE (Piotto et al., 1992) pulse sequence for water signal suppression were collected at 303 K with mixing times of 100 ms and spin-lock times of 90 ms, respectively.

All 2D spectra consisted of 4 K data points in the *F*2 dimension. From 800 to 1024 experiments were recorded in the *F*1 dimension, using 64−192 scans per experiment. Raw data were multiplied in both dimensions by a pure cosine-squared (NOESY, TOCSY) and a pure sine-squared (COSY) bell window function and Fourier-transformed to obtain 2048 × 2048 real data points. A polynomial baseline correction was applied in both directions. The spectra were calibrated assuming chemical shifts of 4.85 and 4.75 ppm for the water signal with respect to 2,2-dimethyl-2-silapentane-5-sulfonate (DSS) at 295 and 303 K, respectively.

Data processing was performed by using a standard Bruker software package. The 2D maps were analyzed on IBM RISC 6000 computers with the program XEASY (ETH, Zürich) (Eccles et al., 1991).

Distance Geometry Calculations. The volumes of the cross-peaks between assigned resonances were obtained using the integration routines present in the program XEASY. Elliptical integration was applied. The dipolar connectivities were taken from the 100-ms NOESY experiment recorded in H_2O solution with presaturation at 303 K. Sometimes two cross-peaks appear degenerate within the spectral resolution in a given map. When their cross-peaks' intensity is given in the supporting information, it means that the splitting of the two cross-peaks has been achieved in another map by changing the temperature or the solvent composition (H_2O/D_2O). Connectivities whose volumes could be better measured in the NOESY spectra recorded either with a presaturation pulse sequence in D_2O solution or with a watergate pulse sequence in H_2O or at a different temperature were scaled referring to a few intraresidue connectivities whose volumes could be accurately measured in all spectra.

NOESY cross-peak intensities were converted into upper limits of interatomic distances by the use of the program CALIBA (Güntert et al., 1991). As previously described by Wüthrich et al. (Wüthrich, 1989; Güntert et al., 1991; Eccles et al., 1991; Güntert & Wüthrich, 1991), the upper limits obtained from CALIBA were classified as: (i) intraresidue except NH, Hα, H*β*; (ii) sequential and intraresidue NH, Hα, H*β*; (iii) medium-range (all non-sequential interresidue connectivities between NH, Hα, H*β* within a segment of five consecutive residues); (iv) long-range backbone; and (v) long-range. For NOEs involving methyl groups, the upper limits were evaluated independently using five analogous classes. All the NOESY cross-peak intensities are reported in the supporting information. The figures of the volumes come from the computer output; their last digits do not have physical meaning. However, the empirical calibration procedures of CALIBA and the use of only upper distance limits remove any effect of these meaningless digits in the following structure calculations. The upper distance constraints were then used to generate protein conformers by using the distance geometry (DG) program DIANA (Güntert et al., 1991).

Upper and lower distance limits were imposed to build up the heme (see the Results for details). In addition, the nonstandard amino acid trimethyllysine present in position 72 was built and added to the DIANA library (Banci et al., 1995).

With the preliminary structures available, the scaling factors for the volume-to-distance conversion for each class were evaluated by plotting volumes of peaks arising from pairs of protons at fixed distance. As the structure emerged from successive runs of DIANA calculations, selected interatomic distances were taken from these structures and additional calibrations were performed. Several cycles of the structure calculation were carried out in order to recalibrate the NOE distance constraints.

DIANA calculations, including the use of the redundant angle strategy routine (REDAC) (Güntert & Wüthrich, 1991), were performed following the procedure and with the parameters already used by us for the determination of other solution structures (Banci et al., 1994, 1995). Initially, 500 random structures were calculated. The final distance geometry calculation on 39 structures was performed without angle constraints to prove convergence. Stereospecific assignments of diastereotopic protons and methyl groups were obtained using the program GLOMSA (Güntert et al., 1991). The average structure calculated from the best 20 structures obtained from DIANA (*vide infra*) was energy minimized and used for comparison with the crystal structures.

Structure Analysis. The structure analysis, in terms of Ramachandran plots, deviation from ideal structural parameters, secondary structure elements, etc., was performed with the PROCHECK program (Laskowski et al., 1993). Visual inspection and drawing of the various families were performed with the program RASMOL (R. Sayle, Biomolecular Structure Department, Glaxo Research and Development, Greenford, Middlesex, U.D., 1994).

RESULTS

Sequence-Specific Assignment

An almost complete sequence-specific assignment of the ^{1}H NMR spectrum of reduced (Cys102Thr) yeast iso-1-cytochrome *c* at 300 K (pH and buffer not reported) is available in the literature (Gao et al., 1990). We have

Table 1: ^{1}H NMR Resonances in Reduced Yeast Iso-1-cytochrome *c* Assigned in This Work[a]

residue	chemical shift (ppm)
Glu 4	NH 7.29
Lys 11	Hγ1 1.45
Leu 15	δ2CH$_3$ 0.97
His 18	Hδ1 9.76
Pro 30	Hδ2 0.13, Hδ1 0.77
Lys 54	Hδ1 1.61, Hγ2 1.55, Hγ1 1.47
Lys 55	Hβ2 1.80
Tyr 67	Hδ1 7.02, Hδ2 7.28, Hϵ1 7.55, Hϵ2 7.75
Tml 72	Hγ1 1.17, Hϵ1 3.06, Hϵ2 3.19
Ile 75	δ1CH$_3$ 1.01
Pro 76	Hβ1 1.75, Hβ2 2.21[b]
Leu 85	Hβ1 1.52, Hβ2 1.63[c]
Lys 87	Hγ1 1.78
Lys 89	Hγ1 1.52, Hγ2 1.61
Arg 91	Hβ2 1.94, Hγ1 1.21, Hγ2 1.75
Tyr 97	Hδ1 6.95, Hϵ1 6.28
Ser 102	NH 7.71, Hα, 4.31

[a] The sample conditions are pH 7.0, 50 mM phosphate buffer. [b] In previous work (Gao et al., 1990) only one Hβ proton was assigned (1.87 ppm). [c] In previous work (Gao et al., 1990) only one Hβ proton was assigned (1.45 ppm).

repeated the assignment for reduced Cys102Ser iso-1-cytochrome *c* under our experimental conditions (50 mM phosphate buffer, pH 7.0) using TOCSY and COSY in H_2O and D_2O for spin patterns and NOESY spectra in H_2O for sequential NH-NH and Hα−NH connectivities.

Our assignment is consistent with that previously published, although we have not been able to confirm the assignment of the protons of Gly 45 and a different assignment has been found for the Hβs of Glu 66. About 30 newly assigned protons are reported in Table 1. The NH of Glu 4 was assigned on the basis of its strong NOE to the NH of Phe 3. The aromatic side chain of Tyr 67 is now completely assigned. The detection of an individual resonance for each proton of the aromatic ring indicates that the side chain is quite rigid, at variance with earlier proposals (Gao et al., 1990; Qi et al., 1994; Moore & Williams, 1980a; Moore & Williams, 1980b; Wand et al., 1989). Thr 5 and Gly 83 remain unassigned. The stereospecific assignment of 60 protons was made by use of the program GLOMSA. The whole assignment is available as supplementary material.

This is an extensive assignment of a large cytochrome (108 amino acids), accounting for 77% of the expected proton resonances: for comparison, 88% of the expected proton resonances have been assigned in reduced cytochrome c_{553} from *Desulfovibrio vulgaris* Hildenborough (79 amino acids) (Marion & Guerlesquin, 1992); 96% in reduced cytochrome c_6 from the green alga *Monoraphidium brauni* (89 amino acids) (Banci et al., 1996); 81% in reduced horse heart cytochrome *c* (103 amino acids) (Wand et al., 1989); and 82% in the cyanide adduct of oxidized Ala 80 yeast cytohrome *c* (Banci et al., 1995).

Information on the Secondary Structure

The amide exchange data and the short and medium-range NOEs observed for the backbone protons in the 100-ms NOESY maps in H_2O are summarized in Figure 1. Sequential NH−NH connectivities for stretches longer than two residues were observed for positions 5−10, 12−19, 27−29, 36−38, 50−55, 61−65, 68−70, 72−75, 79−82, 84−87, 88−92, and 95 to the C-terminus. Sequential connectivities have not been observed for the entire protein due to the presence of four prolines which do not have amide protons (Pro 25, Pro 30, Pro 71, and Pro 76) and three unassigned amide protons (−3, 45, 83). Possible NH−NH connectivities at positions 20, 21, 38, 41, 46, 58, 65, 67, 87, 92, 93 cannot be observed because of nearly degenerate amide proton chemical shifts at positions *i* and *i*+1.

Strong sequential NH−NH NOEs and medium Hα−NH-(*i*,*i*+3) and Hα−NH(*i*,*i*+4) NOEs are indicative of α-helical structures, while the presence of Hα−NH(*i*,*i*+2) indicates the presence of a 3_{10} helical conformation (Wüthrich, 1986). From inspection of Figure 1, it is evident that helical units are present for the segments 5−11, 15−18, 50−55, 61−68, 72−75, and 88−103. The presence of *i*,*i*+2 connectivities in all the helices suggests that they are distorted toward the 3_{10} conformation.

Slowly exchanging backbone amide protons (whose resonances were still detectable a few weeks after the sample had been dissolved in D_2O solution) are also reported in Figure 1. They have been observed for 47 out of 100 residues with assigned amide protons. Most of these protons are involved in helices, where they form H-bonds which prevent them from fast exchange with the bulk solvent. Others are located in the interior of the protein or are involved in other H-bonds.

Solution Structure Determination

A total of 1702 experimental NOE constraints were assigned and integrated and then transformed into upper distance limits using the program CALIBA (Güntert et al., 1991). The number of constraints transformed into upper distance limits is presented in Table 2 for each calibration class. The calibration is in agreement with the volume-to-distance correlation, where the intensities were assumed to be inversely proportional to the sixth power of the corresponding upper distance limits in the case of each class of protons and classes 1, 3, and 5 of methyls and to the fifth power for the class 2 of methyls.

1442 out of 1702 constraints were meaningful and therefore have been taken into account by DIANA. The remaining constraints were found to be irrelevant for the calculation. These latter constraints are meaningless either because they correspond to fixed interproton distances or because they correspond to distances that cannot be violated by any conformation of the polypeptide chain.

The number of NOE constraints per residue is shown in Figure 2. This corresponds to 15.8 NOEs per residue as input for the DIANA calculations and 13.4 accepted experimental constraints per residue. The latter compare with the 14.5 and 13.1 meaningful NOEs per residue used for the structure calculations of cyt c_6 and the cyanide adduct of Ala 80 cyt *c*, respectively. In the case of horse heart cytochrome *c*, a total of 1904 NOEs was used for structure calculation, which corresponds to 18.8 observed NOEs per residue; the number of meaningful NOEs was not reported (Qi et al., 1994). For reduced cytochrome c_{553} from *D. vulgaris* Hildenborough (Marion & Guerlesquin, 1992), 11.1 NOEs per residue were used in the structure determination procedure; again, the number of meaningful constraints was not reported.

The heme, the axial ligands, and the two Cys residues covalently linked to the heme unit were treated as previously reported (Banci et al., 1995, 1996), i.e., including the heme

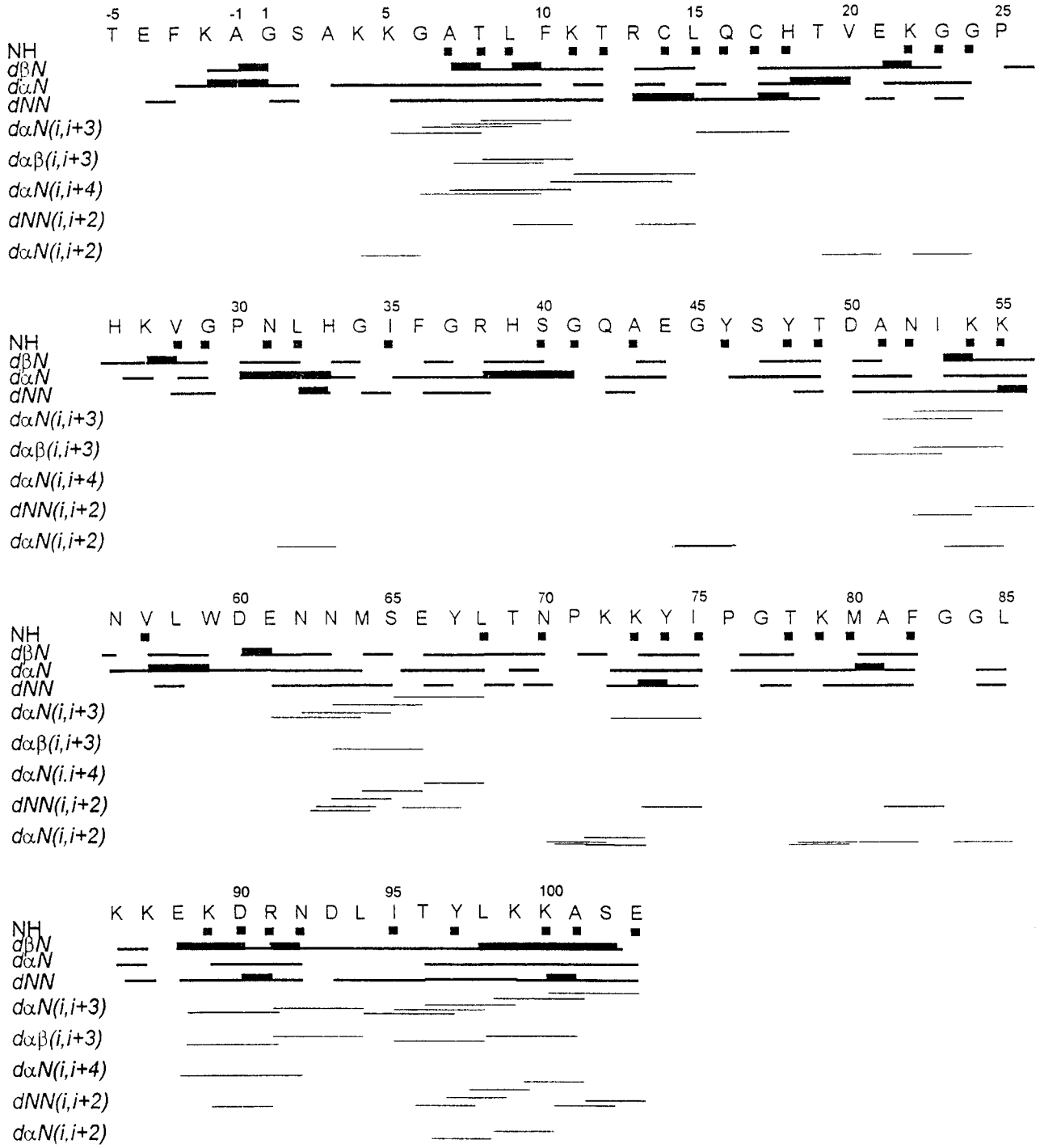

FIGURE 1: Sequential dipolar connectivities involving NH, Hα, and Hβ protons in the reduced form of yeast iso-1-cytochrome *c*. The thickness of the bar indicates the relative NOE intensities. In the first line, NH resonances that were found to exchange slowly in D_2O solution are also indicated by full squares.

Table 2: Number of Cross-Peaks Constituting the Upper Distance Limits File Used in DIANA Calculations on Reduced Yeast Iso-1-cytochrome *c*, Divided According to the Classes Described in the Experimental Section[a]

1	intraresidue (except NH, Hα, Hβ)	389 (151)
2	sequential and intraresidue NH, Hα, Hβ	610 (19)
3	medium-range	92 (1)
4	long-range backbone	18 (−)
5	long-range	593 (295)

[a] The number of cross-peaks involving methyl groups are reported in parentheses.

in the distance geometry calculations through the addition of an artificial amino acid to the residue library used by the program DIANA. The artificial residue consists of a histidine residue whose Nϵ2 was connected to the heme skeleton through links with the four pyrrole nitrogens (upper distance limits 2.9 Å). As the DIANA library does not allow the introduction of metal ions, the heme iron was defined as a dummy atom and its hexacoordinate geometry was simulated by imposing the appropriate upper and lower distance limits between this dummy atom and the ligand atoms. Starting from the four pyrrole nitrogens, the heme skeleton was built by defining covalent bonds between the atoms in such a way that the heme conformation comes out the same as in the X-ray structure of reduced yeast cytochrome *c*. Upper and lower distance limits (2.1 and 1.8 Å,

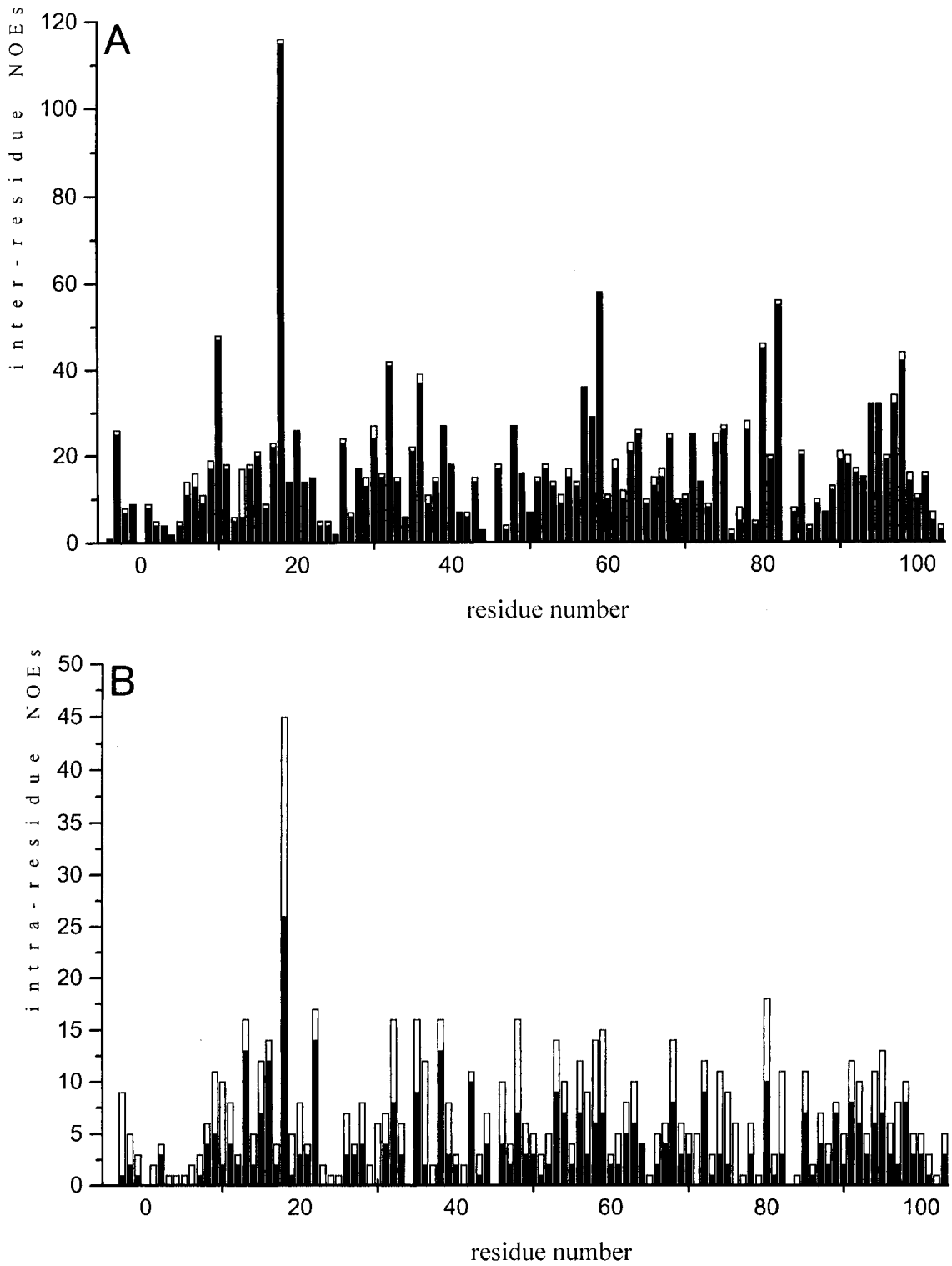

FIGURE 2: Number of (A) inter- and (B) intra- NOEs per residue identified in the NMR spectra. The total height of each column represents the amount of observed experimental NOEs. The open and filled bars correspond to NOE constraints which were found to be irrelevant and meaningful, respectively.

respectively) between the cysteine sulfur and the α-carbon of the corresponding thioether substituent were also used to define the links between Cys 14 and Cys 17 and the heme. An upper distance limit of 2.5 Å and a lower distance limit of 1.8 Å were imposed between the iron and the methionine sulfur atom. Defining the appropriate bonds as rotatable, the heme substituents were allowed to assume all possible conformations. Analogously, the His 18 ring and the Met 80 side chain could change their orientations with respect to the heme plane axes. 500 structures were initially calculated, and 60 stereospecific assignments of diasterotopic protons were obtained through the use of the program GLOMSA.

In the final stages of the distance geometry calculations, hydrogen-bond contraints were also included (Qi et al., 1994; Detlefsen et al., 1991; Markus et al., 1994; Banci et al., 1995, 1996). The geometric criteria we chose for the presence of a hydrogen bond requires the proton−acceptor distance to be less than 2.4 Å and the angle formed by the proton, the donor atom, and the acceptor atom to be within 35°. For

FIGURE 3: Stereodrawing of the 20 best structures of reduced yeast iso-1-cytochrome *c* that constitute the DG family.

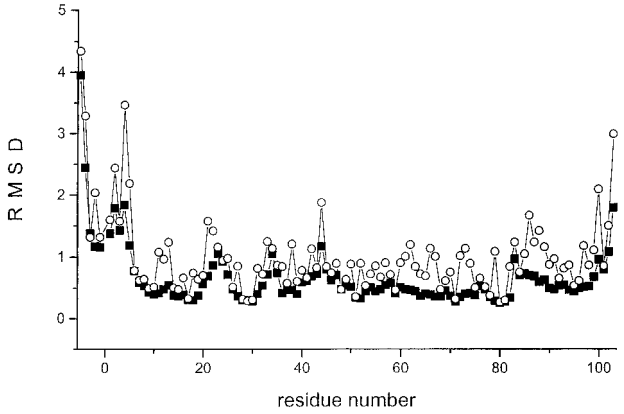

FIGURE 4: Diagrams of the RMSD per residue for the 20 structures of the DG family. RMSD values for the backbone and the heavy atoms are represented by symbols ■ and ○, respectively.

the main chain atoms, these criteria were found to be satisfied in most of the structures by the following 12 NH/CO pairs: Lys 11/Ala 7, Leu 15/Phe 10, Cys 17/Cys 14, His 18/Cys 14, Lys 55/Ile 53, Leu 68/Met 64, Tyr 74/Asn 70, Arg 91/Lys 87, Asn 92/Glu 88, Ile 95/Arg 91, Tyr 97/Asp 93, and Ala 101/Tyr 97. All of these hydrogen bonds involve amide protons that were found to exchange slowly in D_2O solution (see Figure 1). Another H-bond present in all the calculated structures is that between Hδ1 of His 18 and CO of Pro 30. The Hδ1 proton was also found to exchange slowly in D_2O solution. The introduction of hydrogen-bond constraints does not sensibly improve the quality of the structure.

The DG family obtained using constraints derived from dipole−dipole connectivities and hydrogen bonds consists of 20 structures with the lowest values for the target function (i.e., $\leq$0.82 Å^2) and with individual violations of the distance constraints that do not exceed 0.27 Å. A stereodrawing of the DG family (backbone, heme, and its axial ligands) is shown in Figure 3. The distribution of the RMSD per residue within the DG family for both backbone and all heavy atoms is shown in Figure 4 (symbols ■ and ○, respectively). The RMSD values with respect to the mean structure are 0.61 $\pm$ 0.09 Å and 0.98 $\pm$ 0.09 Å for the backbone and all heavy atoms, respectively, when residues 6−100 are considered. The structures constituting the family have an average target function of 0.57 Å^2. The N-terminal residues (−5 to 6) show the largest RMSD values. Substantial disorder for these residues was observed in the X-ray crystal structure of yeast iso-1-cytochrome *c* in both oxidation states (Berghuis & Brayer, 1992); and RMSD values larger than the average are found for the fragments 22−26, 34−36, and 42−47. A slight increase in the spreading of the family is also observed between residue 83 and residue 88. The 48−82 region is well defined, with RMSD values lower than the average. The pattern of the RMSD values per residue compares well with that previously found for the cyanide adduct of oxidized Ala 80 cytochrome *c* (Banci et al., 1995). A trend of the RMSD values similar to that found for the backbone atoms also is observed for the heavy atoms (Figure 4).

The energy-minimized average structure calculated from the above family of 20 structures was used to check the quality of the structure in a Ramachandran plot. The protein contains 90 "meaningful" residues (i.e., non-glycine, non-proline, and non-terminal residues) for the Ramachandran plot. In the energy-minimized average structure, 68 residues (i.e., 75.6% of the meaningful residues) fall in the most favored regions; 19 residues (i.e., 21.1%) are in the additional allowed regions; Arg 13 and Glu 66 fall in the generously allowed regions, while Phe 36 is in the disallowed region.

32 structures were calculated with a target function lower than 1 Å^2. They were all used for further analysis, as they represent a larger ensemble to analyze statistical properties.

Comparison with Related Structures

All of the secondary structural features and the overall folding observed in the X-ray structure are completely maintained in the solution structure. A ribbon diagram of the solution structure is presented in Figure 5. The elements of secondary structure were identified using both a Ramachandran φ, ψ plot and an analysis of the main-chain hydrogen bonding (Table 3). Each of the 32 calculated DG structures was investigated. The observed hydrogen bonds involving main chain atoms confirm the presence of the helices predicted on the basis of the medium-range NOEs (*vide supra*). From the analysis of the structure it is clear that all of the helices observed in the crystal (Berghuis & Brayer, 1992; Louie & Brayer, 1990) are maintained in solution, as observed in the case of the horse heart protein (Qi et al., 1994) and for the cyanide adduct of the Ala 80 mutant (Banci et al., 1995). Moreover, as reported for cytochromes c_{551} (Detlefsen et al., 1991) and c_{553} (Marion & Guerlesquin, 1992; Blackledge et al., 1995), our NMR data are compatible with another helix at positions 15−18. The presence of an analogous helix can also be inferred from the NMR data on the cyanide adduct of oxidized Ala 80 cytochrome *c* (Banci et al., 1995).

There also are hydrogen bonds associated with the tertiary structure. Though present with optimal geometry only in 11 out of 32 structures, the NH of Gly 1 and the side chain oxygen of Thr 96 are consistently within hydrogen-bond

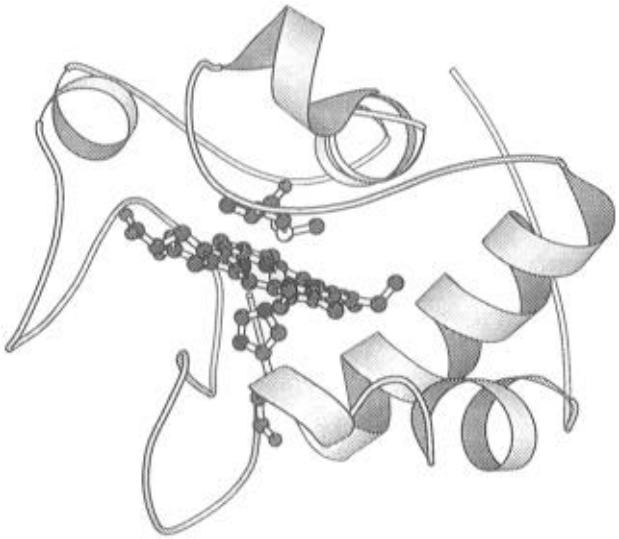

FIGURE 5: Ribbon diagram of the solution structure of reduced yeast iso-1-cytochrome *c*, displayed using MOLSCRIPT (Kraulis, 1991) and Raster3D (Bacon & Anderson, 1988). The structure was obtained from the 20 solution structures of the distance geometry family followed by energy minimization.

Table 3: Hydrogen Bonding between Main Chain Atoms Observed in the 32 Structures of Reduced Yeast Iso-1-cytochrome *c* Obtained from DG Calculations

donor atom	acceptor atom	frequency
NH Gly 1	Oγ1 Thr 96	11
NH Phe 10	CO Gly 6	19
NH Lys 11	CO Ala 7	31
NH Thr 12	CO Leu 9	21
NH Leu 15	CO Phe 10	31
NH Cys 17	CO Cys 14	32
NH His 18	CO Cys 14	32
Hδ1 His 18	CO Pro 30	32
NH Gly 24	CO Lys 22	17
NH Ile 35	CO His 33	13
NH Gly 37	CO Trp 59	25
NH Lys 55	CO Ile 53	32
NH Asp 60	Oδ1 Asn 63	13
NH Ser 65	CO Glu 61	12
NH Glu 66	CO Asn 62	25
NH Tyr 67	CO Asn 63	13
NH Leu 68	CO Met 64	32
NH Lys 69	CO Ser 65	28
NH Asn 70	CO Glu 66	16
NH Tyr 74	CO Asn 70	23
NH Ile 75	CO Pro 71	23
NH Phe 82	CO Met 80	19
NH Arg 91	CO Lys 87	32
NH Asn 92	CO Glu 88	32
NH Asp 93	CO Lys 89	24
NH Leu 94	CO Asp 90	30
NH Ile 95	CO Arg 91	30
NH Thr 96	CO Asn 92	23
NH Leu 98	CO Leu 94	32
NH Lys 99	CO Ile 95	25
NH Lys 100	CO Tyr 97	26
NH Thr 102	CO Leu 98	24
NH Glu 103	CO Lys 100	10

distance, suggesting a tight interaction between the N- and the C-terminal helices. The same hydrogen bond was found in about 20% of the calculated structures of the cyanide adduct of Ala 80 cytochrome *c* (Banci et al., 1995). In the X-ray structure of the reduced form of yeast cytochrome *c*, a hydrogen bond between the NH proton of the Trp 59 indole ring and the O2 atom of the heme propionate was observed (Louie & Brayer, 1990). This hydrogen bond is not observed in the present solution structure of reduced yeast cytochrome *c* nor in the solution structure of reduced horse heart cytochrome *c* (Qi et al., 1994). However, it was observed in the solution structure of the cyanide adduct of the oxidized yeast Ala 80 mutant (Banci et al., 1995). Finally, it is interesting to note that in the X-ray structure of oxidized yeast cytochrome *c*, Trp 59 experiences higher thermal factors than in the reduced form, which suggests a weaker hydrogen bond, with an increased NH−O2 distance (Berghuis & Brayer, 1992). This behavior could indicate that the hydrogen bonds are very sensitive to minor structural rearrangements. The H-bond between the Hδ1 of His 18 and the carbonyl oxygen of Pro 30, described in the crystal structure, is present in all of the calculated structures of the DG family. It also was observed in the case of the cyanide adduct of yeast Ala 80 cytochrome *c* (Banci et al., 1995).

Although the solution structure of the cyanide adduct of oxidized Ala 80 cytochrome *c* (Banci et al., 1995) has the same secondary structure elements found in the solution structure of the reduced form of yeast iso-1-cytochrome *c*, different exchange rate patterns were observed for the amide protons. Compared to the 47 slowly exchanging amide protons in the present structure, only 26 were found in the oxidized mutant (Banci et al., 1995). Whereas the distribution of slowly exchanging amides in the two proteins is almost the same in the first and last helices, a larger number of slowly exchanging NHs in the helices present between 50 and 75 are found in the present case. Moreover, two other areas characterized by slowly exchanging NHs, not observed in the Ala 80 protein, are present between residues 28 and 35 and residues 78 and 82. The latter segment contains the mutated residue and it has been shown that replacement of the axial Met 80 with an Ala creates a large "distal" cavity (Banci et al., 1995). Therefore, a different solvent accessibility to these residues around the mutation site cannot be ruled out. The former segment and the three helices in the 50−75 residue range are, however, well removed from the mutation site. An increase in hydrogen exchange rates has been observed on going from the reduced (ferrous) to the oxidized (ferric) state of horse heart cytochrome *c* by infrared (Kagi & Ulmer, 1968; Ulmer & Kagi, 1968) and NMR spectroscopy (Patel & Canuel, 1976; Wand et al., 1986). It is therefore tempting to propose that the observed differences are related to the different dynamical features of the two redox states of the protein. This hypothesis is supported by some preliminary results on the oxidized form of yeast iso-1-cytochrome *c* (unpublished results of this lab).

Looking at specific protein sites which are thought to be significant for biological function, we have compared the energy-minimized mean structure ⟨DG⟩ with the X-ray structure of the free reduced yeast iso-1-cytochrome *c* (hereafter referred to as red cyt *c*) (Louie & Brayer, 1990) and with that of the cytochrome in the complex with yeast cytochrome *c* peroxidase (Pelletier & Kraut, 1992) (where the cytochrome *c* is oxidized; hereafter referred to as ox cyt *c*:CcP). The pairwise RMSD values are reported in Table 4. For the backbone atoms the largest differences between solution and X-ray structures are observed at positions −5, −4, −2, 2−4, 11, 12, 21−26, 38, 41−44, 60, and 103 for the uncomplexed cytochrome *c* and at positions −5, −4, −2, −1, 2−4, 8, 12, 22−25, 37, 38, 41−44, 57, 58, and 103 for the complex. Most of these residues correspond to those

Table 4: RMSD Values for the Backbone (Upper Diagonal) and All Heavy Atoms (Lower Diagonal) of the Energy-Minimized Average Solution Structure of Reduced Yeast Iso-1-cytochrome *c* (⟨DG⟩) with Respect to the X-ray Crystal Structures of Reduced Yeast Iso-1-cytochrome *c* (red cyt *c*) (Louie & Brayer, 1990) and of the Yeast Iso-1-cytochrome *c* Complexed to Cytochrome *c* Peroxidase (ox cyt *c*:CcP) (Pelletier & Kraut, 1992)[a]

	⟨DG⟩	red cyt *c*	ox cyt *c*:CcP	⟨Ala 80⟩
⟨DG⟩	–	0.87	0.90	1.00
red cyt *c*	1.62	–	0.40	0.98
ox cyt *c*:CcP	2.46	2.00	–	0.97
⟨Ala 80⟩	1.47	1.51	2.39	–

[a] A comparison with the energy-minimized average solution structure of the cyanide adduct of the Ala 80 mutant of cytochrome *c* (⟨Ala 80⟩) (Banci et al., 1995) is also given.

with the largest RMSD values within the family and probably the differences are not very meaningful. Concerning all the heavy atoms (hereafter referred to as HA), the solution structure is closer to the crystal structure of the reduced free cytochrome *c* than to that of the oxidized cytochrome *c* in the complex. This is not a surprising result. However, there are meaningful discrepancies from this global value in some particular residues.

A few side chains have been proposed to be relevant in the intermolecular contacts with CcP (Pelletier & Kraut, 1992). An analysis of the conformation of these residues in the various structures is reported in Table 5. The Gln 16 side chain changes conformation in the complex, as compared to free cytochrome *c*, folding back to form a hydrogen bond with its own backbone amide nitrogen, thus allowing larger access to heme pyrrole ring C. Asn 70, Lys 73, and Lys 87 could serve as potential H-donors in hydrogen bonds with negatively charged residues on the CcP surface, although some rearrangement of the side chains is required for either of the two partner molecules with respect to the X-ray structure of the complex to allow formation of these hydrogen bonds. The predominant forces holding the complex together are hydrophobic and van der Waals interactions involving Leu 9, Arg 13, Ala 81, Phe 82, Gly 83, and Lys 86 on cytochrome *c*. We have therefore focused our attention on these side chains. Gln 16 in the solution structure is well defined (RMSD of 0.67 Å for the all heavy atoms), and its side chain conformation is closer to that of ox cyt *c*:CcP in the crystal than to that of the free red cyt *c* in the crystal (RMSD values for all heavy atoms of 1.36 and 2.15 Å, respectively). Of the residues which could serve as H-bond donors, Asn 70 shows RMSD values for the heavy atoms within the family lower than the average (i.e., 0.76 Å), whereas Lys 73 and Lys 87 are less defined [RMSD(HA) of 1.14 and 1.24 Å, respectively]. However, in the average structure the latter has a conformation not too different from that observed in both crystal structures [RMSD(HA) = 1.04−1.05 Å]. Lys 73 is almost superimposable in the present solution structure and in the crystal structure of red cyt *c* [RMSD(HA) = 0.96 Å], while it has a different orientation in ox cyt *c*:CcP [RMSD(HA) = 1.67 and 1.66 Å with reference to the solution and the crystal, respectively]. Asn 70 in the three structures does not differ substantially; its position in the ox cyt *c*:CcP is intermediate between that observed in solution [RMSD (HA) = 0.85 Å] and that found in the crystal of the free red cyt *c* [RMSD(HA) = 0.51 Å].

Among the residues involved in van der Waals interactions, Leu 9 and Ala 81 are both very well defined in the solution structure [RMSD(HA) within the DG family of 0.50 and 0.30 Å]. The latter residue has an almost identical arrangement in the three structures, whereas the former is slightly different in solution. The Phe 82 ring also is characterized within the DG family by RMSD values lower than the average; its position in the two crystal structures is not too different [RMSD(HA) = 1.49 Å], but the conformation in the average structure in solution is the same as that in ox cyt *c*:CcP [RMSD(HA) = 0.30 Å]. Gly 83 and the side chain of Lys 86 are poorly defined in the solution structure: the former residue is not assigned, and only the βCH_2 protons have been identified for the side chain of Lys 86. Nevertheless, the Gly 83 conformation does not differ too much in the three structures, the solution structure being closer to that of ox cyt *c*:CcP. On the other hand, the side chain of Lys 86 has a very similar position in the two crystal structures but largely different in the solution structure. Due to the lack of experimental data on this side chain, the difference could be meaningless. Substantial differences between the solution structure, on one side, and the two crystal structures, on the other, also are observed for the Arg 13 side chain, which shows RMSD values within the family only slightly larger than the average and which is defined by a reasonable number of NOEs.

From the comparison of all these structures with the solution structure of the cyanide adduct of oxidized Ala 80 cytochrome *c* (Table 4), we can see that the overall structure of the oxidized mutant is much closer to the structure of the

Table 5: Pairwise RMSD Values between the Average Solution Structure of Reduced Yeast Iso-1-cytochrome *c* (⟨DG⟩) and the X-ray Crystal Structures of Reduced Yeast Iso-1-cytochrome *c* (red cyt *c*) (Louie & Brayer, 1990) and of Yeast Iso-1-cytochrome *c* Complexed to Cytochrome *c* Peroxidase (ox cyt *c*:CcP) (Pelletier & Kraut, 1992)[a]

residue	⟨DG⟩/red cyt *c*	⟨DG⟩/ox cyt *c*:CcP	red cyt *c*/ox cyt *c*:CcP	⟨DG⟩/⟨Ala 80⟩	red cyt *c*/⟨Ala 80⟩	ox cyt *c*:CcP/⟨Ala 80⟩
Gln 16	2.15	1.36	2.23	1.17	1.50	1.64
Asn 70	1.20	0.85	0.51	1.13	1.86	1.51
Lys 73	0.96	1.67	1.66	1.29	1.74	1.93
Lys 87	1.04	1.05	1.10	2.82	2.85	2.30
Leu 9	1.31	1.65	0.68	1.81	1.60	1.39
Arg 13	2.10	2.07	0.70	1.90	1.80	1.93
Ala 81	0.32	0.52	0.28	0.65	0.75	0.99
Phe 82	1.54	0.30	1.49	1.10	1.23	1.04
Gly 83	1.09	0.85	0.42	1.36	1.92	1.61
Lys 86	2.93	3.02	0.69	1.86	1.98	1.83

[a] calculated for all heavy atoms for residues that have been proposed to be involved in the interaction with cytochrome *c* peroxidase. A comparison with the energy-minimized average solution structure of the cyanide adduct of the Ala 80 mutant of cytochrome *c* (⟨Ala 80⟩) (Banci et al., 1995) is also given.

reduced form both in solution and in the crystal than to that of the ox cyt *c*:CcP crystal. However, if we analyze the residues involved in complex formation in the cyanide adduct of oxidized Ala 80 cytochrome *c*, they are closer to the ox cyt *c*:CcP than to the red cyt *c* crystal, as found for the solution structure of reduced yeast iso-1-cytochrome *c*.

Concluding Remarks

The solution structure of reduced yeast cytochrome *c* has been obtained through dipolar couplings involving 539 assigned protons out of 703. For a nonenriched protein (enrichment being infeasible with the expression system in use) this is a significant achievement. The average RMSD of the family is relatively high although the structure is well resolved in large parts of the protein. The observability of a large number of amide NHs in D_2O solution indicates a relative rigidity of the backbone as opposed to the cyanide adduct of the oxidized Ala 80 protein, which shows a smaller number of slowly exchanging signals. An additional helix involving residues 15−18, which was not reported for the crystal structure, is detected in solution. The overall folding seen in the X-ray structure is maintained in solution. The hydrogen-bond network is maintained between the crystal and solution structures. When the residues involved in the interaction with cytochrome *c* peroxidase are considered, in many cases in solution they are closer to the crystalline complex than to the crystalline free molecule.

SUPPORTING INFORMATION AVAILABLE

Table containing proton assignments for reduced yeast cytochrome *c* (shift values measured at 303 K) and a listing of the experimental NOESY intensities as well as the hydrogen-bond constraints used for the structure calculation (72 pages). Ordering information is given on any current masthead page.

REFERENCES

Bacon, D. J., & Anderson, W. F. (1988) *J. Mol. Graph. 6*, 219−220.

Banci, L., Bertini, I., Eltis, L. D., Felli, I. C., Kastrau, D. H. W., Luchinat, C., Piccioli, M., Pierattelli, R., & Smith, M. (1994) *Eur. J. Biochem. 225*, 715−725.

Banci, L., Bertini, I., Bren, K. L., Gray, H. B., Sompornpisut, P., & Turano, P. (1995) *Biochemistry 34*, 11385−11398.

Banci, L., Bertini, I., Quacquarini, G., Walter, O., De la Rosa, M. A., & Navarro, M. (1996) *JBIC 1*, 330−340.

Bax, A., & Davis, D. G. (1985) *J. Magn. Reson. 65*, 355−360.

Berghuis, A. M., & Brayer, G. D. (1992) *J. Mol. Biol. 223*, 959−976.

Blackledge, M. J., Medvedeva, S., Poncin, M., Guerlesquin, F., Bruschi, M., & Marion, D. (1995) *J. Mol. Biol. 245*, 661−681.

Detlefsen, D. J., Thanabal, V., Pecoraro, V. L., & Wagner, G. (1991) *Biochemistry 30*, 9040−9046.

Eccles, C., Güntert, P., Billeter, M., & Wüthrich, K. (1991) *J. Biomol. NMR 1*, 111−130.

Eden, D., Matthew, J. B., Rosa, J. J., & Richards, F. M. (1982) *Proc. Natl. Acad. Sci. U.S.A. 79*, 815−819.

Feng, Y., & Englander, S. W. (1990) *Biochemistry 29*, 3505−3509.

Feng, Y., Roder, H., & Englander, S. W. (1990) *Biochemistry 29*, 3494−3504.

Gao, Y., Boyd, J., Williams, R. J. P., & Pielak, G. J. (1990) *Biochemistry 29*, 6994−7003.

Griesinger, C., Otting, G., Wüthrich, K., & Ernst, R. R. (1988) *J. Am. Chem. Soc. 110*, 7870−7872.

Güntert, P. (1992) *DIANA Program Version 2.1, User's Manual and Instructions*, Institut fuer Molekularbiologie und Biophysik Eidgenoessische Technische Hochschule, Hoenggerberg, CH-8093 Zürich, Switzerland.

Güntert, P., & Wüthrich, K. (1991) *J. Biomol. NMR 1*, 447−456.

Güntert, P., Braun, W., & Wüthrich, K. (1991) *J. Mol. Biol. 217*, 517−530.

Kagi, J. H., & Ulmer, D. D. (1968) *Biochemistry 7*, 2718.

Korszun, Z. R., Moffatt, K., Frank, K., & Cusanovich, M. A. (1982) *Biochemistry 21*, 2253−2258.

Kraulis, P. J. (1991) *J. Appl. Crystallogr. 24*, 946−950.

Laskowski, R. A., MacArthur, M. W., Moss, D. S., & Thornton, J. M. (1993) *J. Appl. Crystallogr. 26*, 283−291.

Liu, G., Crygon, C. A., & Spiro, T. G. (1989) *Biochemistry 28*, 5046−5050.

Louie, G. V., & Brayer, G. D. (1990) *J. Mol. Biol. 214*, 527−555.

Lu, Y., Casimiro, D. R., Bren, K. L., Richards, J. H., & Gray, H. B. (1993) *Proc. Natl. Acad. Sci. U.S.A. 90*, 11456−11459.

Macura, S., Wüthrich, K., & Ernst, R. R. (1982) *J. Magn. Reson. 47*, 351−357.

Marion, D., & Wüthrich, K. (1983) *Biochem. Biophys. Res. Commun. 113*, 967−974.

Marion, D., & Guerlesquin, F. (1992) *Biochemistry 31*, 8171−8179.

Markus, M. A., Nakayama, T., Matsudaira, P., & Wagner, G. (1994) *Protein Sci. 3*, 70−81.

Moore, G. R. (1983) *FEBS Lett. 161*, 171−175.

Moore, G. R., & Williams, R. J. P. (1980a) *Eur. J. Biochem. 103*, 513−522.

Moore, G. R., & Williams, R. J. P. (1980b) *Eur. J. Biochem. 103*, 523−532.

Moore, G. R., & Pettigrew, G. W. (1990) *Cytochromes c: Evolutionary, Structural and Physicochemical Aspects*, Springer-Verlag, Berlin.

Patel, D. J., & Canuel, L. L. (1976) *Proc. Natl. Acad. Sci. U.S.A. 73*, 1398.

Pelletier, H., & Kraut, J. (1992) *Science 258*, 1748−1755.

Pettigrew, G. W., & Moore, G. R. (1987) *Cytochromes c: Biological Aspects*, Springer-Verlag, Berlin.

Piotto, M., Saudek, V., & Sklenar, V. (1992) *J. Biomol. NMR 2*, 661−666.

Qi, P. X., Di Stefano, D. L., & Wand, A. J. (1994) *Biochemistry 33*, 6408−6417.

Rance, M., Sørensen, O. W., Bodenhausen, G., Wagner, G., Ernst, R. R., & Wüthrich, K. (1983) *Biochem. Biophys. Res. Commun. 117*, 479.

Trehwella, J., Carlson, V. A. P., Curtis, E. H., & Heidorn, D. B (1988) *Biochemistry 27*, 1121−1125.

Ulmer, D. D., & Kagi, J. H. (1968) *Biochemistry 7*, 2710.

Wagner, G. (1990) *Prog. Nucl. Magn. Reson. Spectrosc. 22*, 101−139.

Wand, A. J., Roder, H., & Englander, S. W. (1986) *Biochemistry 25*, 1107−1114.

Wand, A. J., Di Stefano, D. L., Feng, Y., Roder, H., & Englander, S. W. (1989) *Biochemistry 28*, 186−194.

Wüthrich, K. (1986) *NMR of Proteins and Nucleic Acids*, Wiley, New York.

Wüthrich, K. (1989) *Acc. Chem. Res. 22*, 36−44.

Wüthrich, K. (1995) *Acta Crystallogr. D51*, 249−270.

BI961110E